European Polymer Journal 45 (2009) 3043–3057

Contents lists available at ScienceDirect

European Polymer Journal

journal homepage: www.elsevier.com/locate/europolj

Preparation, characterization and hydrolytic degradation of poly[*p*-dioxanone-(butylene succinate)] multiblockcopolymer

Song-Dong Ding *, Guang-Can Zheng, Jian-Bing Zeng, Li Zhang, Yi-Dong Li, Yu-Zhong Wang **

Center for Degradable and Flame-Retardant Polymeric Materials (ERCEPM-MoE), College of Chemistry, State Key Laboratory of Polymer Materials Engineering, Sichuan University, Chengdu 610064, People's Republic of China

ARTICLE INFO

Article history:
Received 21 April 2009
Received in revised form 21 August 2009
Accepted 23 August 2009
Available online 27 August 2009

Keywords:
Poly(*p*-dioxanone)
Poly(butylene succinate)
Poly[*p*-dioxanone-(butylene succinate)]
Hydrolytic degradation

ABSTRACT

A series of poly[*p*-dioxanone-(butylene succinate)] (PPDOBS) copolymers were prepared from *p*-dioxanone (PDO), 1,4-butanediol and succinate acids through a two-step process including the initial prepolymer preparation of poly(*p*-dioxanone)diol (PPDO-OH) and poly(butylene succinate)diol (PBS-OH) and the following copolymerization of the two kinds of prepolymers by coupling with hexamethylene diisocyanate (HDI). The molecular structures of the prepared PPDO-OH, PBS-OH and PPDOBS were characterized by hydrogen nuclear magnetic resonance spectroscopy (^{1}H NMR). The crystallization of the copolymers was investigated by using differential scanning calorimetry (DSC), polarized optical microscopy (POM) and wide angle X-ray diffraction (WAXD). It has been shown that the crystallization rate and the degree of crystallization increases with the increase of the weight fraction of poly(butylene succinate) (PBS) blocks in the copolymers. In phosphate buffer solution with pH 7.4 at 37 °C for 18 weeks, the hydrolytic degradation behaviors of the copolymers were studied. The changes of retention weight, water absorption, pH value, and surface morphologies with the degradation time showed that the hydrolytic degradation rate of PPDOBS could be controlled by adjusting the weight fraction of poly(*p*-dioxanone) (PPDO) and PBS blocks in the copolymers. The changes of the thermal properties of PPDOBS during the degradation were also investigated by DSC.

1. Introduction

Poly(*p*-dioxanone) (PPDO), a biodegradable aliphatic poly(ether-ester), has attracted more and more attentions for its excellent biodegradability, biocompatibility and bioabsorbability [1]. It has been used in medical field such as sutures, surgery repair materials and drug delivery systems [2–4]. In recent years, owing to the great progress on the catalytic synthesis technology of *p*-dioxanone (PDO) monomer from diethylene glycol [5], the production cost of PDO as well as its polymer PPDO decreased significantly. At present, PPDO has been considered as a candidate not only for medical uses but also for universal uses, such as films, molded products, laminates, foams, non-woven material, adhesives and coatings [6–8]. However, due to its poor thermal stability, low crystallization rate, as well as sensitivity to moisture, the applications of PPDO are limited greatly [9–16]. Therefore, it is very important for PPDO to be modified.

As a common and an effective method, copolymerization is often employed to improve the properties of polymer. In recent years, there were some reports on the copolymerization for PPDO with other aliphatic polyesters [17–22]. The copolymerization was carried out through three main methods as follows: the direct ring-opening copolymerization of PDO with other lactone; the ring-opening polymerization of PDO in the presence of macroinitiator; and the copolymerization of PPDO and other prepolymer by coupling with diisocyanate. Generally

* Corresponding author. Tel./fax: +86 28 85410259.
** Corresponding author.
E-mail addresses: dsd68@163.com (S.-D. Ding), yzwang@scu.edu.cn (Y.-Z. Wang).

0014-3057/$ - see front matter © 2009 Elsevier Ltd. All rights reserved.
doi:10.1016/j.eurpolymj.2009.08.019

speaking, by using the former two methods, only the copolymer with low molecular weights can be obtained. For the direct ring-opening copolymerization, due to the significant difference in reactivity between PDO and the other lactone such as ε-caprolactone, glycolide and lactide, high molecular weight copolymers are difficult to be obtained [17]. For the ring-opening polymerization in the presence of macroinitiator, it is only under the condition of the very low molar ratio of the macroinitiator to PDO (macroinitiator/PDO) that the copolymers obtained can have high molecular weight. However, in that case, the content of macroinitiator is too low to attain the aim of modifying PPDO. Higher molar ratio of macroinitiator/PDO is good for the copolymerization, but the copolymers obtained only have low molecular weight because of the existence of more active species. Li et al. [18] prepared poly(lactic acid-b-*p*-dioxanone) block copolymers from ring-opening polymerization of PDO in the presence of poly(L-lactic acid) (PLA) macroinitiators. The highest intrinsic viscosity of the block copolymers was only 0.97 dL/g. In addition, it was found that it was difficult to induce the ring-opening polymerization of PDO and no copolymer was obtained when the molar fraction of PLA exceeded 60%. For the copolymerization by coupling, high molecular weight copolymers can be easily obtained through the reaction of poly(*p*-dioxanone)diol with other dihydroxyl-terminated prepolymers using diisocyanate as chain-extender. The corresponding studies mainly focus on the copolymerization of PPDO and poly-ε-caprolactone (PCL) [21,22]. Lendlein et al. [22] developed shape-memory copolymers with high molecular weight via coupling oligo(*p*-dioxanone)diol and oligo(ε-caprolactone)diol with 2,2(4),4-trimethylhexanediisocyanate. The thermally induced shape-memory property at the temperature of about 40 °C endows this kind of copolymers with potential values in biomedical field, especially in smart degradable sutures applications. However, due to the sensitivity to temperature in dimensional stability, the thermally induced shape-memory property hampers greatly the applications as the universal materials, especially as environment-friendly materials. In order to widen the scope of the applications of PPDO, it is necessary to use another aliphatic polyesters to improve its properties through copolymerization.

As one of the most representative and generally acknowledged biodegradable aliphatic polyester, poly(butylene succinate) (PBS), which has good degradability and excellent melt processability, has been used extensively [23–25]. Compared with PCL, PBS has a much higher melting point of 112–114 °C. It is expected that the copolymer of PPDO and PBS may have better dimension stability at ambient temperature and more extensive applications than the copolymer of PPDO with PCL. Besides the excellent properties mentioned above, PBS is also a polymer with slow degradation rate by hydrolysis. Therefore, a combination with the fast hydrolysable polymer PPDO can allow the design of a range of new materials with different life times.

With respect to the copolymerization of PPDO and PBS, Zhang et al. [20] developed a novel biodegradable copolymer from chain-extension of PPDO with PBS. It was found that PPDO had good compatibility with PBS, and the copolymer had better thermal stability than PPDO. However, there are some defects with respect to the synthetic method. For a coupling agent for hydroxyl-adding type of toluene-2,4-diisocyanate (TDI), in order to obtain high molecular weight copolymer, the coupling reaction must be carried out at high temperature (180 °C) for long time (6 h) because of none dihydroxyl-terminated prepolymers of both PPDO and PBS. In that case, the resulting copolymers were not only deeply colored but also seriously cross-linked, and there were little values in practical applications. In order to avoid those shortcomings, a new synthetic route was presented. In the present paper, poly[*p*-dioxanone-(butylene succinate)] (PPDOBS) copolymers with higher molecular weight were prepared through a two-step process including the initial prepolymer preparation of poly(*p*-dioxanone)diol and poly(butylene succinate)diol and the following copolymerization of the two kinds of prepolymers by coupling with hexamethylene diisocyanate (HDI). The molecular structures of the prepared poly(*p*-dioxanone)diol, poly(butylene succinate)diol and the copolymer PPDOBS were characterized by ^{1}H NMR. The crystallization of PPDOBS was investigated by using DSC, POM and WAXD. In addition, a hydrolysis degradation was performed in phosphate buffer solution with pH 7.4 at 37 °C and the water absorption, retention weight, pH value, thermal properties, and surface morphologies were monitored during the degradation process.

2. Experimental

2.1. Materials

p-Dioxanone (PDO), provided by the Pilot Plant of the Center for Degradable and Flame-Retardant Polymeric Materials (Chengdu, China), was dried over CaH_2 for 48 h and distilled under reduced pressure before use. Stannous octoate (⩾95%) and tetrabutyl titanate (AR grade) were purchased from Sigma (USA) and Kelong Chemical Corporation (Chengdu, China), respectively, and used as received. After diluted with anhydrous toluene, $SnOct_2$ solution and $Ti(OBu)_4$ solution were stored in the glass ampoules under nitrogen. 1,6-Hexamethylene diisocyanate (AR grade) from Sigma (USA), 1,4-butanediol (AR grade) and succinic acid (AR grade) from Zhiyuan Chemical Company (Tianjin, China) were used without further purification. All other chemicals with AR grades were used as received.

2.2. Preparation of dihydroxyl-terminated prepolymers

Poly(*p*-dioxanone)diol (PPDO-OH) prepolymer was prepared through bulk ring-opening polymerization of PDO using 1,4-butanediol (BD) as an initiator, and $SnOct_2$ as a catalyst. The preparation was performed in a flame-dried glass reactor with magnetic stirring. The reactor was evacuated and purged with nitrogen three times prior to addition of PDO and BD with syringe. The molar ratio of PDO to BD was fixed at 40. The reactor was immersed into an oil bath at 80 °C with stirring for 10 min. Then $SnOct_2$ solution was injected into the reactor using the molar ratio of BD to $SnOct_2$ with 1000. After 72 h at 80 °C, the reactor was cooled down rapidly to room

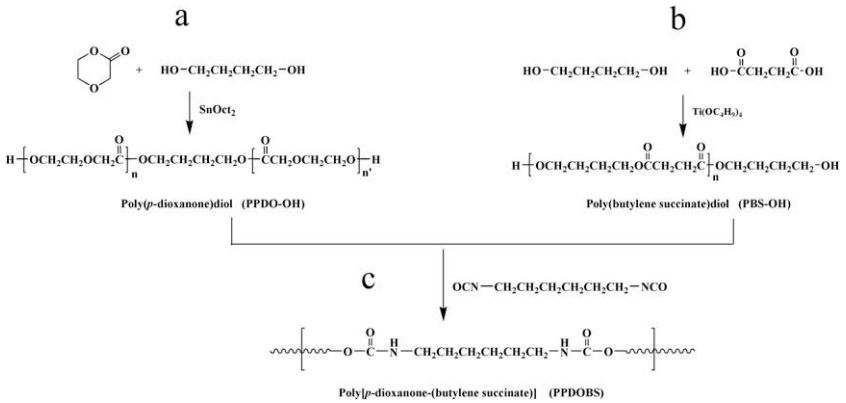

Scheme 1. Preparation route for PPDO-OH (a), PBS-OH (b), and PPDOBS (c).

temperature. The product obtained was milled into small chips, then dried under vacuum at 40 °C to a constant weight and stored in a desiccator over silica gel. The preparation route for PPDO-OH was shown in Scheme 1a.

Poly(butylene succinate)diol (PBS-OH) prepolymer was prepared via a two-step procedure including esterification and following polycondensation. First, 1.0 mol succinic acid and 1.2 mol 1,4-butanediol were added into a 500 mL three-necked round-bottom flask equipped with a mechanical stirrer, a Dean–Stark water separator and a nitrogen inlet pipe. The esterification was carried out at 200 °C for 4 h. Then, the catalyst tetrabutyl titanate with 0.1 wt.% of the total amount of reactants was introduced into the flask with a syringe. The polycondensation was continued at 230 °C with vacuum of 30 Pa for 2 h. The viscous liquid product was cooled down to room temperature under nitrogen flow. The resulting polymer was milled into small chips, then dried under vacuum at 40 °C to a constant weight and stored in a desiccator over silica gel. The preparation route for PBS-OH was shown in Scheme 1b.

2.3. Preparation of poly[p-dioxanone-(butylene succinate)] (PPDOBS) copolymers

PPDOBS copolymers were prepared by coupling PPDO-OH and PBS-OH with 1,6-hexamethylene diisocyanate (HDI). The preparation route was shown in Scheme 1c. The coupling reaction was performed in bulk using a glass reactor under nitrogen atmosphere. PPDO-OH and PBS-OH were added into the reactor equipped with a mechanical stirrer and a nitrogen inlet pipe. The reactor was evacuated and purged with nitrogen three times. Then the reactor was immersed into a silicone oil bath at 160 °C. When the prepolymers were melted completely, HDI was injected with a syringe into the reactor using the molar ratio of HDI to the total amount of the prepolymers with 1.1. The coupling reaction proceeded for 1 h with a continuous nitrogen flow. Then the reactor was cooled down rapidly to room temperature. The copolymer obtained was milled into small chips, then dried under vacuum at 40 °C to a constant weight and stored in a desiccator over silica gel.

2.4. Characterization

2.4.1. Gel permeation chromatography (GPC)

The molecular weights of PPDO-OH and PBS-OH prepolymers were determined at 35 °C by GPC, using a Waters GPC device equipped with a 1515 pump, a Waters model 717 autosampler, and a 2414 refractive index detector. Chloroform was employed as the eluent at a flow rate of 1.0 mL/min, and a sample concentration of 2.5 mg/mL was used. The number and weight average molecular weights ($M_{n,GPC}$ and $M_{w,GPC}$, respectively) were calculated by using a calibration curve which was obtained by monodisperse polystyrene standards.

2.4.2. Intrinsic viscosity

As the conventional solvents such as chloroform and tetrahydrofuran used in GPC measurement can not dissolve PPDOBS, only the intrinsic viscosity ($[\eta]$) of 0.1% w/v solution of PPDOBS in phenol/1,1,2,2-tetrachloroethane (1:1 v/v) was measured at 25 °C in a constant temperature water bath using an Ubbelohde viscometer. Prior to measurement, the solution was filtered through a quantitative filter paper.

2.4.3. Nuclear magnetic resonance (NMR) spectroscopy

^{1}H NMR spectra were recorded with a Varian Inova 400 spectrometer and performed at ambient temperature with 5% (w/v) polymer solution in $CDCl_3$ for prepolymers and in DMSO for PPDOBS, and tetramethylsilane was used as the internal reference. The number-average molecular weights ($M_{n,NMR}$) of PPDO-OH and PBS-OH were calculated from the NMR analysis.

2.4.4. Wide angle X-ray diffraction (WAXD)

WAXD experiments were conducted with Cu Kα radiation on a Philips X'Pert Pro X-ray apparatus (Holland). The equipment was operated at 40 kV and 35 mA under room tempeture, and the scan range was between 2° and 50° with a scan rate of 2°/min.

2.4.5. Differential scanning calorimeter (DSC)

DSC measurement was performed with Q100 apparatus (TA Corporation, USA) in sealed aluminum pan under

nitrogen atmosphere. The samples were quickly heated to 140 °C, kept for 5 min to eliminate the thermal history, and then cooled to −50 °C at a cooling rate of 10 °C/min. The samples were again heated up to 140 °C at the same rate. The glass transition temperature (T_g), melting enthalpies, and the melting temperature (T_m) were obtained from the thermogram.

2.4.6. Polar optical microscopy (POM)

POM was carried out with a Nikon ECLIPSE LV 100POL microscope in conjunction with a hot stage (HSC621V). Samples were melted in glass slides with cover slips to form thin films. The specimens were heated to 140 °C on a hot plate holding for 3 min and then quickly cooled to the required crystallization temperature. The growth of spherulites was recorded on a video cassette recorder.

2.5. Hydrolytic degradation

The hydrolytic degradation tests were carried out in a phosphate buffer solution with pH 7.4 at 37 °C. The films, which were prepared by compression molding at 140 °C first and then cooled at room temperature rapidly, were cut into 20 × 10 mm^2 slabs with a thickness of 0.5 mm. Before immersed in the buffer solution, each sample was weighed on a Mettler analytical balance (AL204). Three samples were taken out of the hydrolysis medium and rinsed with distilled water to remove the phosphate every week. After wiping, the three samples were weighed first and then dried under vacuum at ambient temperature to constant weight. Before continuing the experiment, the buffer solution was renewed. Total remaining weight and water absorption were calculated from the following relationships: retention weight% = m_t/m_0, water absorption% = $(m_w - m_t)/m_t$, where m_0 and m_t represented the initial and remaining weights of the dried samples, and m_w represented the wet weight of the samples after wiping. The values of the retention weight and water absorption were given by means of the average measurement value of the three samples. pH changes were measured by a Leici pH meter (PHS-3C). SEM evaluation was carried out to examine the surface morphology of the samples by using JSM-5900LV (JEOL Corporation, Japan). DSC analysis was used to determine the changes in thermal characteristics of the samples with the hydrolysis time.

3. Results and discussion

3.1. Preparation of PPDO-OH and PBS-OH prepolymers

By reference to the literature [26], the dihydroxyl-terminated PPDO-OH prepolymer was prepared via ring-opening polymerization of PDO by using 1,4-butanediol as an initiator and $SnOct_2$ as a catalyst. The molecular structure of PPDO-OH was characterized by ^{1}H NMR, and the spectrum was shown in Fig. 1a. The resonance signals belonging to the three kinds of methylene protons in the repeating PPDO units were observed at 4.16 (δH^a), 3.78 (δH^b) and 4.33 (δH^c) ppm. The shifts occurring at 1.71 (δH^d) and 4.12 (δH^e) ppm with the same integral area were assigned to the methylene protons of BD, while the shifts observed at 3.76 ($\delta H^{b'}$) and 3.68 ($\delta H^{c'}$) ppm were ascribed to the methylene protons connecting with the terminal hydroxyl groups. From the data of ^{1}H NMR, the number-average molecular weight of PPDO-OH ($M_{n,NMR}$) can be calculated according to the following equation:

$$M_{n,NMR} = 102 \times \frac{I_{4.33} + I_{3.68}}{I_{3.68}} + 88 + 2 \quad (1)$$

where $I_{4.33}$ and $I_{3.68}$ were the peak intensities of the corresponding methylene protons, the values of 102, 88, and 2 were the molecular weights of the repeating unit of PPDO, -$OCH_2CH_2CH_2CH_2O$-, and two hydrogen protons at the ends of the molecular chain, respectively. $M_{n,NMR}$ of PPDO-OH prepolymer obtained by ^{1}H NMR is listed in Table 1. By using GPC, the molecular weights of PPDO-OH were also determined (shown in Table 1). $M_{n,GPC}$ of PPDO-OH was much higher than $M_{n,NMR}$. This difference may be ascribed to the different measurement method. Between $M_{n,NMR}$ and $M_{n,GPC}$, it was found that $M_{n,NMR}$ was very effective to determine the amount of coupling agent [27,28]. Therefore, in the following coupling reaction, $M_{n,NMR}$ was employed to calculate the use level of HDI.

The dihydroxyl-terminated PBS-OH prepolymer was prepared by the polycondensation of succinic acid with excessive 1,4-butanediol using $Ti(OBu)_4$ as a catalyst [29]. Fig. 1b shows the ^{1}H NMR spectrum of PBS-OH. Besides the typical proton resonance signals belonging to the repeating units of PBS at 4.13 (δH^e), 2.64 (δH^f) and 1.74 (δH^d) ppm, the proton resonance signal occurring at 3.67 (δH^g) ppm can be assigned to the methylene protons connecting with the terminal hydroxyl groups. No additional carboxyl group resonance signal was detected within the instrumental limit. By ^{1}H NMR analysis, the number-average molecular weight of PBS-OH can be obtained according to the following equation:

$$M_{n,NMR} = 172 \times \frac{I_{4.10}}{I_{3.65}} + 89 + 1 \quad (2)$$

where $I_{4.10}$ and $I_{3.65}$ were the peak intensities of the corresponding methylene protons, the values of 172, 89, and 1 were the molecular weights of the repeating unit of PBS, -$OCH_2CH_2CH_2CH_2OH$, and the hydrogen proton at the end of the molecular chain, respectively. The values of $M_{n,NMR}$ and $M_{n,GPC}$ are listed in Table 1. Just like PPDO-OH, PBS-OH has also the much higher value of $M_{n,GPC}$ than that of $M_{n,NMR}$.

3.2. Preparation of PPDOBS copolymers

PPDOBS copolymers with different composition were prepared via coupling reaction of PPDO-OH with PBS-OH by using HDI as a coupling agent at 160 °C for 1 h. Compared with the reaction conditions used by Zhang et al. [20], the reaction time was much shorter and the reaction temperature was also lower. This is good for the coupling reaction. In order to obtain better insight into the copolymers, the homopolymer only containing PPDO or PBS was also prepared by using PPDO-OH or PBS-OH as the single prepolymer to react with HDI, and remarked as PPDO-H

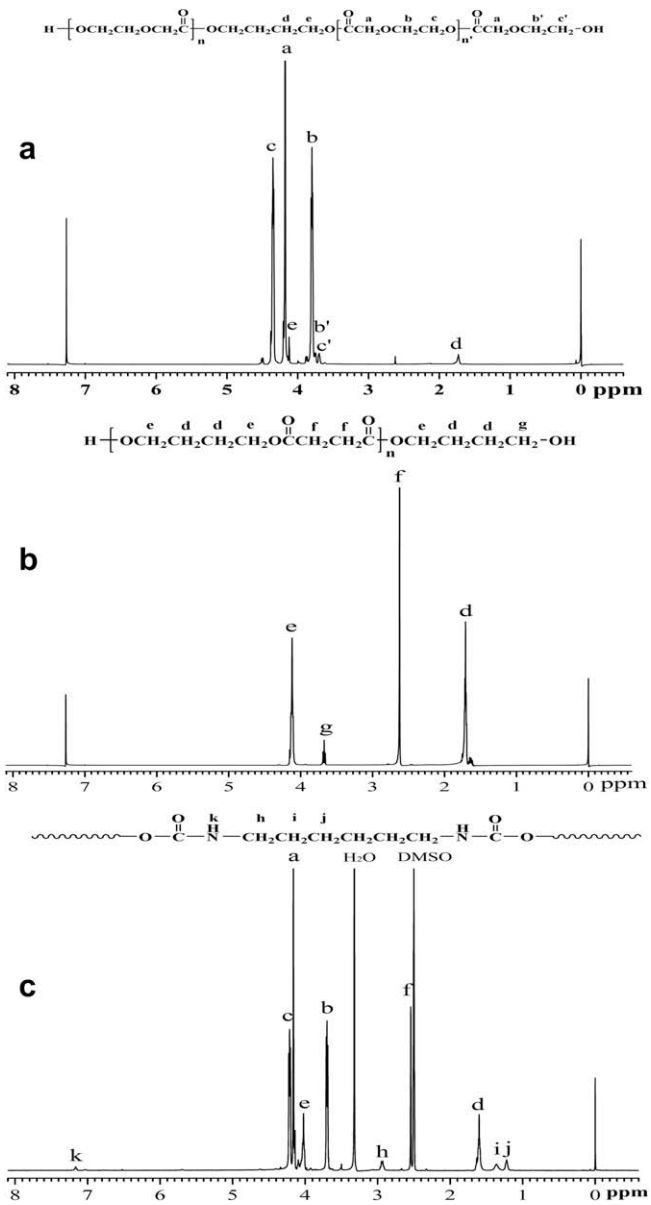

Fig. 1. ^{1}H NMR spectra of PPDO-OH (a), PBS-OH (b), and PPDOBS7 (c).

Table 1
Molecular weights of the prepared PPDO-OH and PBS-OH prepolymers.

Prepolymer	$[\eta]^{a}$ (dL/g)	$M_{n,NMR}{}^{b}$ (g/mol)	$M_{n,GPC}{}^{c}$ (g/mol)	$M_{w,GPC}{}^{c}$ (g/mol)	PDI^{c}
PBS-OH	0.25	3500	6600	12,000	1.78
PPDO-OH	0.22	6600	13,300	18,400	1.39

[a] Measured by Ubbelohde viscometer in phenol/1,1,2,2-tetrachloroethane (1:1 v/v) at 25 °C.
[b] Calculated by ^{1}H NMR.
[c] Determined by GPC in chloroform at 35 °C.

and PBS-H, respectively. The weight fractions of PPDO in PPDOBS copolymers varied from 20 to 90 wt.%. The samples containing 20, 50, 70 and 90 wt.% PPDO are denoted as PPDOBS2, PPDOBS5, PPDOBS7 and PPDOBS9, respectively. The structure of the copolymer was characterized by ^{1}H NMR. Fig. 1c indicates the ^{1}H NMR spectrum of PPDOBS7. It was found that the characteristic chemical shifts ascribed to PPDO (δH^{a}, δH^{b} and δH^{c}) and PBS (δH^{d},

Table 2
Intrinsic viscosity of PPDO-H, PBS-H and PPDOBS copolymers.

Sample	PPDO-H	PPDOBS9	PPDOBS7	PPDOBS5	PPDOBS2	PBS-H
F_{PBS}[a] (wt.%)	0	10	30	50	80	100
$[\eta]$[b] (dL/g)	3.14	3.53	2.86	2.08	3.53	3.75

[a] Weight fraction of PBS blocks in the copolymers.
[b] Measured by Ubbelohde viscometer in phenol/1,1,2,2-tetrachloroethane (1:1 v/v) at 25 °C.

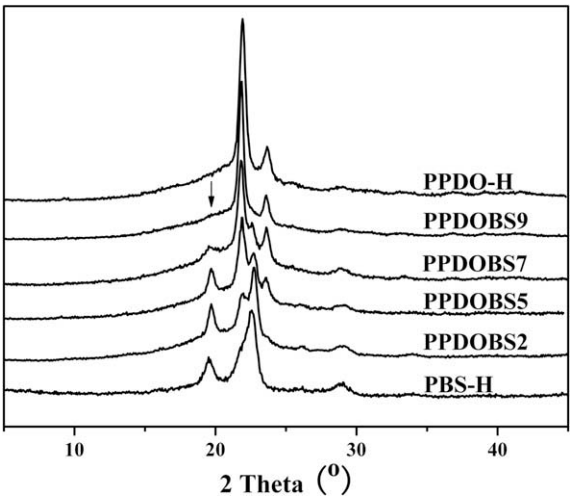

Fig. 2. WXRD diffraction patterns of PPDO-H, PBS-H, and PPDOBS copolymers.

δH^e and δH^f) still occurred in the ^1H NMR spectrum of PPDOBS7. In addition, the shifts of three kinds of methylene protons of HDI, as well as the proton in –NH– group were observed at 1.22 (δH^j), 1.36 (δH^i), 2.94 (δH^h) and 7.20 (δH^k) ppm. After coupling reaction, the shifts at 3.65, 3.76 and 3.68 ppm ascribed to the methylene protons connecting with the terminal hydroxyl of prepolymers disappeared, indicating that the coupling reaction proceeded completely.

Regretfully, GPC measurement of the copolymers can not be performed due to the poor solubility of PPDOBS in the conventional solvents such as chloroform and tetrahydrofuran. Only the intrinsic viscosities ($[\eta]$) of the resulting polymers were measured for a relative comparison, and the corresponding data were listed in Table 2. The intrinsic viscosities of the resulting polymers are more than 10 times higher than those of the prepolymers, indicating that the coupling reaction is very effective.

3.3. Thermal properties and crystallization of PPDOBS copolymers

WAXD was employed to investigate the crystal structures of the samples. The WXRD diffraction patterns of PPDOBS, as well as PBS-H and PPDO-H samples are shown in Fig. 2. It can be seen that both PPDO-H and PBS-H have two obvious diffraction peaks at 2θ of 21.9°, 23.6°, and 19.6°, 22.8°, respectively. With respect to PPDOBS9, although the weight fraction of PBS blocks is only 10 wt.%, a weak diffraction peak originating from PBS blocks at 2θ of 19.6° can still be detected. The X-ray diffraction peaks at 2θ of 21.9°, 23.6°, 19.6°, and 22.8° originating from PPDO and PBS blocks appear also in the other copolymers. This result revealed that PBS and PPDO blocks in the copolymers formed the well self-assembled crystal structures corresponding to PBS-H and PPDO-H types. In addition, the peaks for PPDOBS were less sharp than those of PBS-H and PPDO-H. From PPDOBS9 to PPDOBS2, the peak intensities of PPDO blocks became weaker with increasing the weight fraction of PBS blocks, while those of PBS blocks varied in the opposite direction.

The spherulitic morphologies of the samples were investigated by POM. When PPDO-H and PBS-H crystallized from melt, they formed well-defined spherulites that can exhibit Maltese crosses extinction pattern between crossed polars, which depends on the crystallization temperature and time. Fig. 3a shows the optical micrograph of PPDO-H after isothermal crystallization at 60 °C for 5 min, and Fig. 3b indicates the optical micrograph of PBS-H after isothermal crystallization at 70 °C

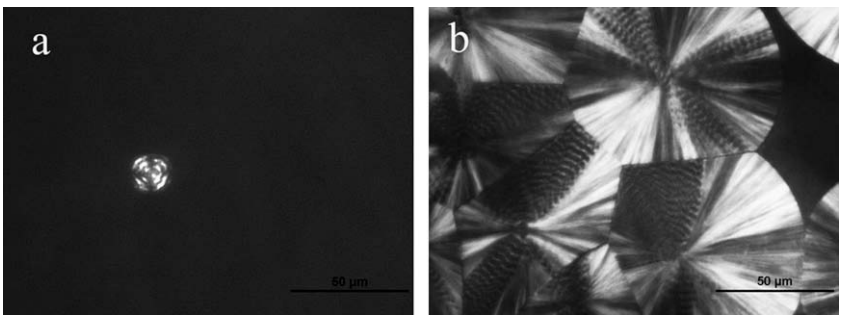

Fig. 3. POM micrographs of PPDO-H (a) crystallizing at 60 °C for 5 min, and PBS-H (b) crystallizing at 70 °C for 1 min.

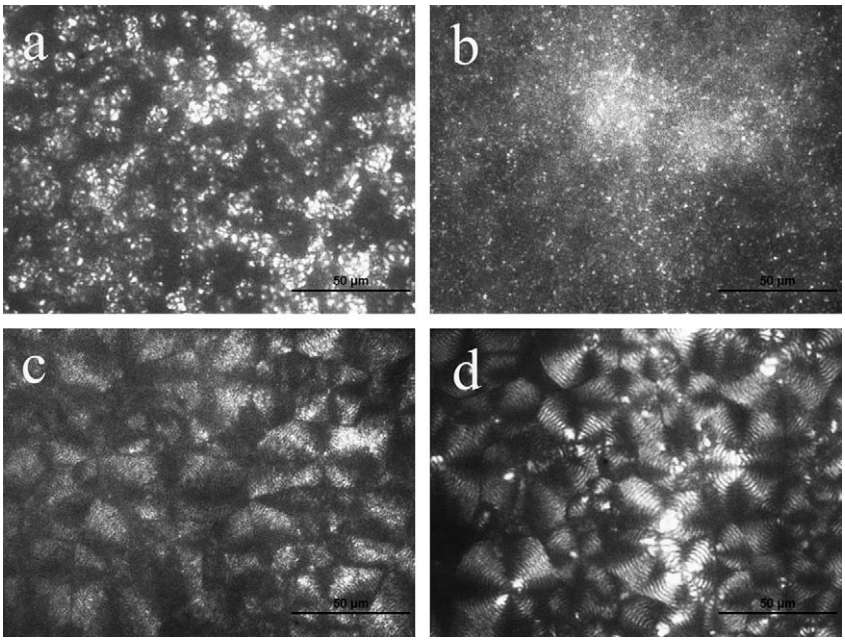

Fig. 4. POM micrographs of PPDOBS copolymers crystallizing at 60 °C for various time: (a) PPDOBS9, for 5 min; (b) PPDOBS7, for 1 min; (c) PPDOBS5, for 0.5 min; (d) PPDOBS2, for 0 min.

for 1 min. Obviously, the crystallization rate of PBS-H was much higher than that of PPDO-H even at higher temperature.

It is well known that there are two key factors that control the overall crystallization rate, one is the nucleation and the other is the crystal growth [30]. Nucleation is a decreasing function of temperature; however, crystal growth is an increasing function of temperature. When the temperature is appropriate, the rates of nucleation and crystal growth are both high enough, the crystallization rate reaches the maximum. Due to the high crystallization rate of PBS, it can be expected that PPDOBS copolymers have higher crystallization rate than PPDO-H, which will be discussed later.

The average spherulite size also depends on the rate of nucleation and growth. When more nuclei are present, more spherulites are formed and the spherulite size becomes smaller at the end of the crystallization process [31]. Fig. 4 shows the optical micrographs of PPDOBS obtained from the isothermal crystallization at 60 °C for various time. All micrographs display the typical Maltese crosses, and the nucleation densities of PPDOBS copolymers are much higher than that of PPDO-H (Fig. 3a). From Fig. 3a, Fig. 4a, and Fig. 4b, it can be observed that the average spherulite size gradually decreases from PPDO-H to PPDOBS9 and to PPDOBS7, while the corresponding nucleation density increases in the same order, implying that PBS blocks play a role of nucleation. Similar nucleating effect in PPDO-b-PCL diblock copolymers was reported by Albuerne et al. [32,33], who found that both PPDO and PCL blocks can crystallize in a supercooling range during the isothermal crystallization. PPDO blocks crystallized first and nucleated PCL blocks. Therefore, the trend of decreasing first and then increasing with increasing the weight fraction of PBS blocks in the average spherulite size of PPDOBS copolymers, which can be observed in Fig. 4, can be attributed to the crystallization of PBS blocks that provide different amounts of nuclei. With increasing the weight fraction of PBS blocks from 10 to 30 wt.%, the more crystalline PBS blocks acted as the nucleating agents, and so the average spherulite size decreased. However, when the weight fraction of PBS blocks exceeded 50 wt.%, the self-crystallization of PBS blocks was dominant, resulting in a decrease of the amounts of nuclei for PPDO blocks crystallization. As a result, the average spherulites size of PPDOBS5 and PPDOBS2 increased.

When the weight fraction of PBS blocks increased from 10 to 80 wt.%, the crystallization rate of the copolymers increased in the order of PPDOBS9, PPDOBS7, PPDOBS5 and PPDOBS2. This result shows that the crystallization rate of the copolymer increases with increasing the weight fraction of the PBS blocks. This is mainly ascribed to the high crystallization rate of PBS blocks and the significant nucleating effect of the crystalline PBS blocks.

The thermal properties of PPDO-H, PBS-H, and PPDOBS were studied by DSC. The DSC curves are shown in Fig. 5. The glass transition temperature (T_g), melting point (T_m), and melting enthalpy (ΔH_m) evaluated from the heating scan are listed in Table 3. The degrees of crystallization (X_c) of PPDO and PBS blocks are also given, which are calculated from the following equation:

$$X_C = \frac{\Delta H_m}{\Delta H^0_{mA} \times A(wt\%)} \quad (3)$$

where $\Delta H_m{}^0{}_A$ is the melting enthalpy per gram of the polymer in its completely crystalline state ($\Delta H_m{}^0{}_{PPDO}$ = 141 J/g

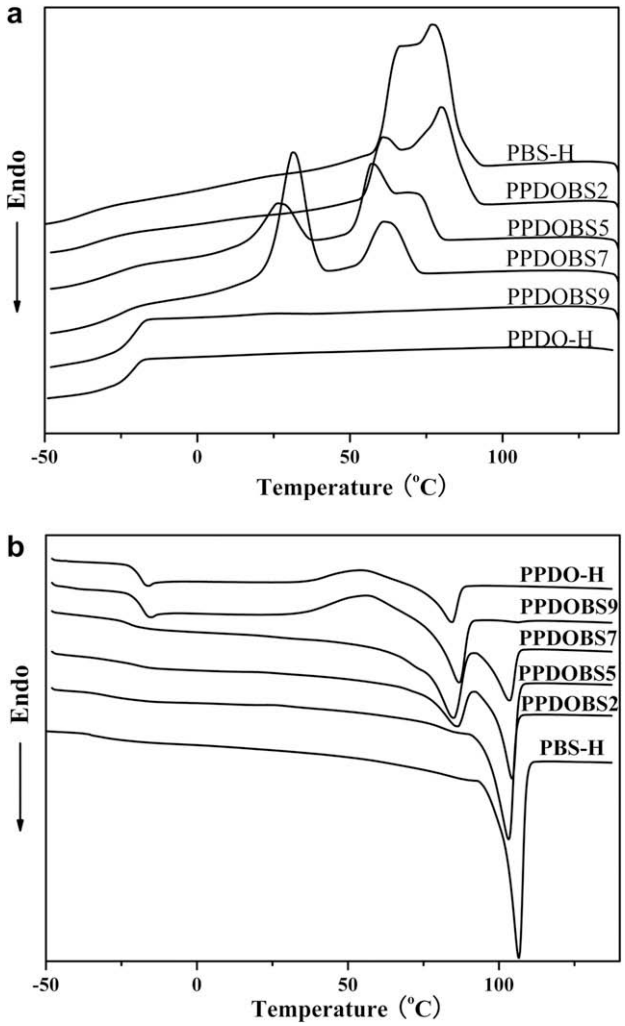

Fig. 5. DSC curves of PPDO-H, PBS-H, and PPDOBS copolymers: (a) cooling scan and (b) heating scan.

Table 3
DSC data of PPDO-H, PBS-H and PPDOBS copolymers obtained from the heating curves.

Sample	T_g (°C)	T_m[a] (°C)	ΔH_m[a] (J/g)	X_c[a] (%)	T_m[b] (°C)	ΔH_m[b] (J/g)	X_c[b] (%)
PPDO-H	−18.0	84.4	11.3	8.0	–	–	–
PPDOBS9	−17.2	86.8	14.5	11.4	106.3	0.3	2.7
PPDOBS7	−22.4	84.8	24.6	24.9	103.5	10.3	31.2
PPDOBS5	−20.0	85.9	13.5	19.1	104.3	19.0	34.5
PPDOBS2	−30.0	84.8	–	–	103.2	26.0	45.4
PBS-H	−35.0	–	–	–	106.6	35.0	47.3

[a] The value of PPDO blocks in the copolymer.
[b] The value of PBS blocks in the copolymer.

[34], $\Delta H_m{}^0{}_{PBS}$ = 110 J/g [35]) and A (wt.%) is the mass percent of the A component.

From Fig. 5, it can be observed that all DSC curves of PPDOBS showed only one glass transition regardless of the composition. The occurrence of a single glass transition step indicated that the amorphous chain ascribed to PBS and PPDO blocks were mixed well, thus leading to the formation of a miscible amorphous phase. In addition, two melting peaks were detected in the heating curves (Fig. 5b), which suggested that both PPDO and PBS blocks crystallized and formed two different crystal domains in PPDOBS copolymers. These results are in good agreement with those obtained from WAXD analyses.

When the weight fraction of PBS blocks exceeded 10 wt.%, the samples displayed the crystallization peaks in the cooling scan and no crystallization peak was detected

in the heating scan, indicating the complete crystallization during the cooling process. It has been shown that the crystallization rate of PPDOBS copolymer increased with increasing the weight fraction of PBS blocks. This result is in accordance with that obtained from POM analyses.

The crystallization peaks of PBS blocks appeared over the temperature of 50 °C during the cooling process (Fig. 5a) and shifted gradually to the higher temperature with increasing the weight fraction of PBS blocks. The corresponding crystallization enthalpy also increased. This may be attributed to the increase in crystallization capacity of PBS blocks with increasing PBS content. With respect to PPDOBS9, in which the weight fraction of PBS blocks was only 10 wt.%, the crystallization enthalpy was so small that the crystallization peak was not appeared on the DSC curve during the cooling process. For PPDOBS7, PPDOBS5, PPDOBS2, and PBS-H, in which the weight fraction of PBS blocks increased from 30 to 100 wt.%, the X_c of PBS blocks gradually increased from 31.2% to 47.3% (Table 3), while the X_c of PBS blocks in PPDOBS9 was only 2.7%.

From Table 3, it can also be seen that all copolymers had a single T_g, which fell between the glass transitions of −18.0 °C for PPDO-H and −35.0 °C for PBS-H. The shift of T_g indicates that PPDO and PBS could be miscible in the amorphous phase. Otherwise, two T_gs corresponding to each polymer would be detected. In addition, the T_ms of both PPDO and PBS blocks were remained and changed slightly, indicating that the composition of PPDOBS had little or no effect on T_m of the copolymers.

The X_c of PPDO blocks in the copolymers increased from 8.0% to 24.9% with increasing the weight fraction of PBS blocks from 0 to 30 wt.%. With the further increase to 50 wt.%, the X_c of PPDO blocks decreased to 19.1%. This decrease was in good accordance with the variation of the crystallization enthalpy of PPDO blocks from PPDOBS7 to PPDOBS5 during the cooling process (Fig. 5a). When the weight fraction of PBS blocks reached to 80 wt.%, the melting peak of PPDO blocks nearly disappeared. From PPDO-H to PPDOBS2, the trend of increasing first and then decreasing in the X_c of PPDO blocks was just opposite to that of decreasing first and then increasing in the average spherulite size measured by POM. This can be also ascribed to the changes in nucleating effect of the crystalline PBS blocks. When the weight fraction of PBS blocks was low, the crystallization of PBS blocks acted as the nuclei for PPDO blocks crystallization, and the X_c of PPDO blocks increased with increasing the weight fraction of PBS blocks. While the weight fraction of PBS blocks increased to 50 wt.%, the self-crystallization of PBS blocks is dominant, and the crystallization of PPDO blocks was confined. As a result, the X_c of PPDO blocks decreased.

As can be seen from the results obtained by WAXD, POM and DSC, PBS blocks crystallize first and then nucleate for PPDO blocks crystallization, and the crystallization rate of PPDO blocks increases with increasing the weight fraction of PBS blocks.

3.4. Hydrolytic degradation

3.4.1. Degradation

In order to investigate the hydrolysis behaviors of PPDOBS copolymers, the hydrolytic degradation was carried out in a phosphate buffer solution with pH 7.4 at 37 °C.

As is well known, the biodegradability of aliphatic polyesters depends mainly on their chemical structures, especially on the hydrolysable ester bonds in the main chains which are susceptible to water attacks. When the samples are in contact with the aqueous medium, water absorption is the first thing. After water diffuses into the samples, hydrolysis of ester bonds begins. As the hydrolysis proceeds, the fragments of low molecular chains which are soluble in the hydrolysis medium produce. When the degraded fragments diffuse and dissolve in the aqueous medium, a weight loss of the samples and decrease of pH of the solution occurs. At the same time, the migration of fragments encourages the absorption of water as water fills

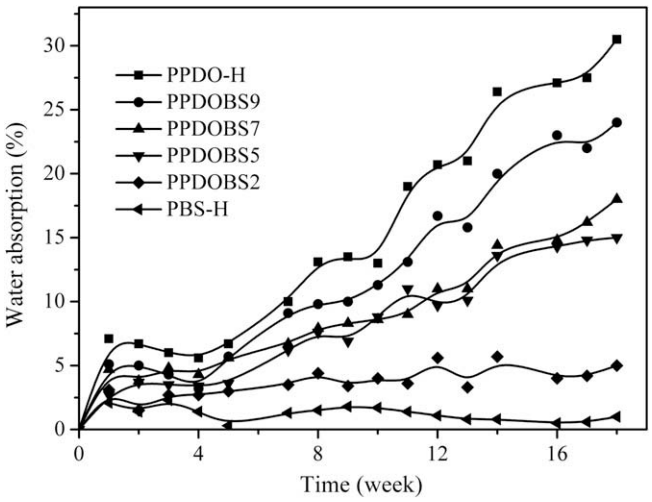

Fig. 6. Variation of water absorption during the hydrolysis of PPDO-H, PBS-H, and PPDOBS copolymers in the phosphate buffer solution (pH 7.4) at 37 °C as a function of hydrolysis time.

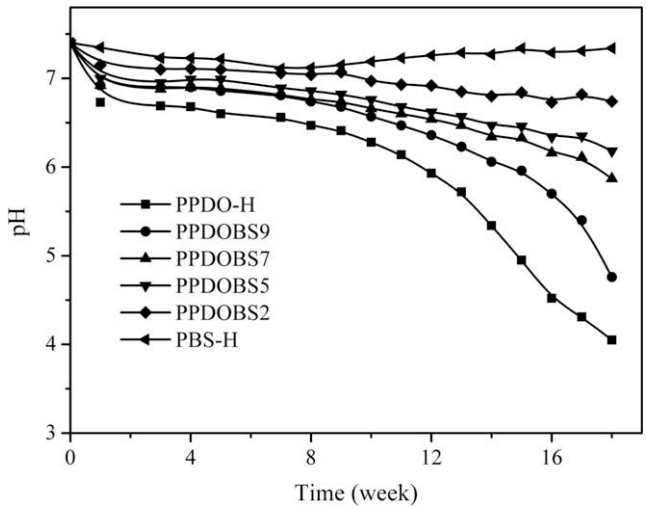

Fig. 7. Variation of solution pH during the hydrolysis of PPDO-H, PBS-H, and PPDOBS copolymers in phosphate buffer solution (pH 7.4) at 37 °C as a function of hydrolysis time.

the spaces left behind. Due to the different chemical structure of PPDO and PBS blocks, the copolymer with various composition will exhibit different degradation properties during the hydrolysis.

Fig. 6 shows the evolution of water absorption with the degradation time. As can be seen, the water absorption profiles of the samples increased as the degradation proceeded. There was a dramatic increase of water absorption for PPDO-H from 4th week to 18th week and 31 ± 2% of water absorption had attained after 18 weeks, while the water absorption of PBS-H varied within 3% for 18 weeks. In the same time span, PPDOBS9, PPDOBS7, PPDOBS5 and PPDOBS2 had the final water absorption of 24 ± 2, 18 ± 2, 15 ± 1 and 5 ± 1%, respectively. The water absorption of PPDOBS copolymers decreased with increasing the weight fraction of PBS blocks, and varied between the water absorption of PBS-OH and PPDO-OH.

The pH value of buffer solution was monitored and the results are shown in Fig. 7. With the increase of hydrolysis time, pH values of the samples decreased. With respect to PPDO-H, the pH value decreased slowly in the first few weeks, but after the initial 4 weeks, it decreased rapidly and a sharp drop occurred from 12th to 18th week, and a final pH value of 4.05 was obtained after 18 weeks. Similar results had been observed for PPDO [36,37]. While the pH value of PBS-H decreased so slowly that no significant change was observed, and the final pH value was only 7.34. With respect to PPDOBS copolymers, the pH value decreased slower than that of PPDO-H, and increased regularly with increasing the weight fraction of PBS blocks,

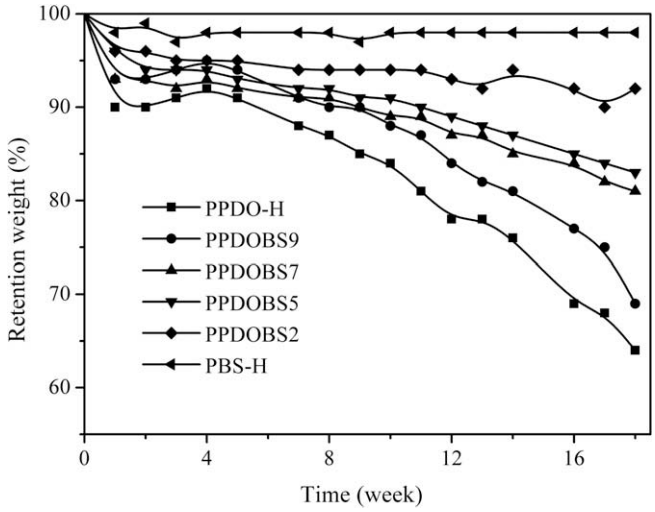

Fig. 8. Variation of retention weight during the hydrolysis of PPDO-H, PBS-H, and PPDOBS copolymers in phosphate buffer solution (pH 7.4) at 37 °C as a function of hydrolysis time.

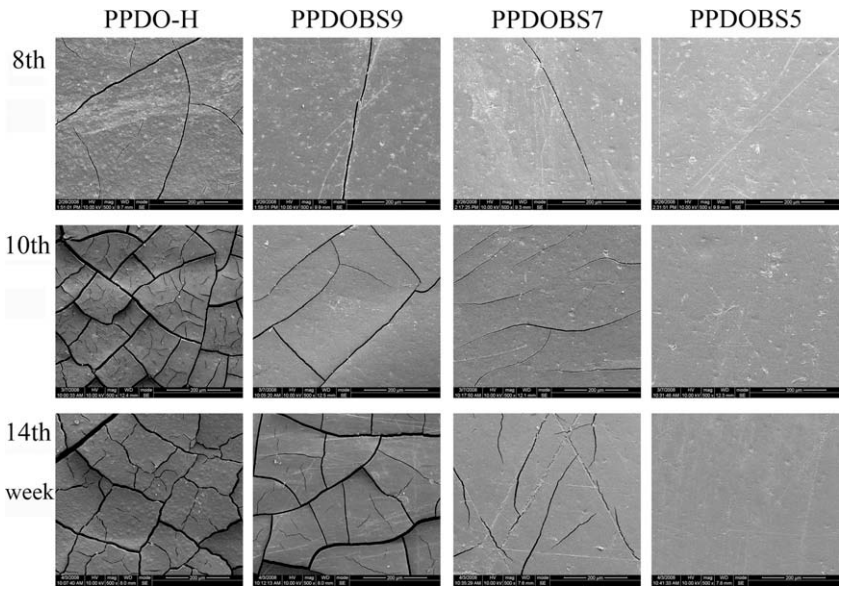

Fig. 9. SEM micrographs of PPDO-H, PPDOBS9, PPDOBS7 and PPDOBS5 (magnification: 500×) during the hydrolysis in phosphate buffer solution (pH 7.4) at 37 °C after 8, 10 and 14 weeks.

which is in concordance with the water absorption results shown in Fig. 6. pH value of the copolymers varied between that of PPDO-H and PBS-H, and the final pH value regularly increased from 4.76 to 6.74 after 18 weeks when the weight fraction of PBS blocks increased from 10 to 80 wt.%. The decrease of pH value suggested that the hydrolysis of the samples produces acid molecules with low molecular weight. It is also seen from the drop that the

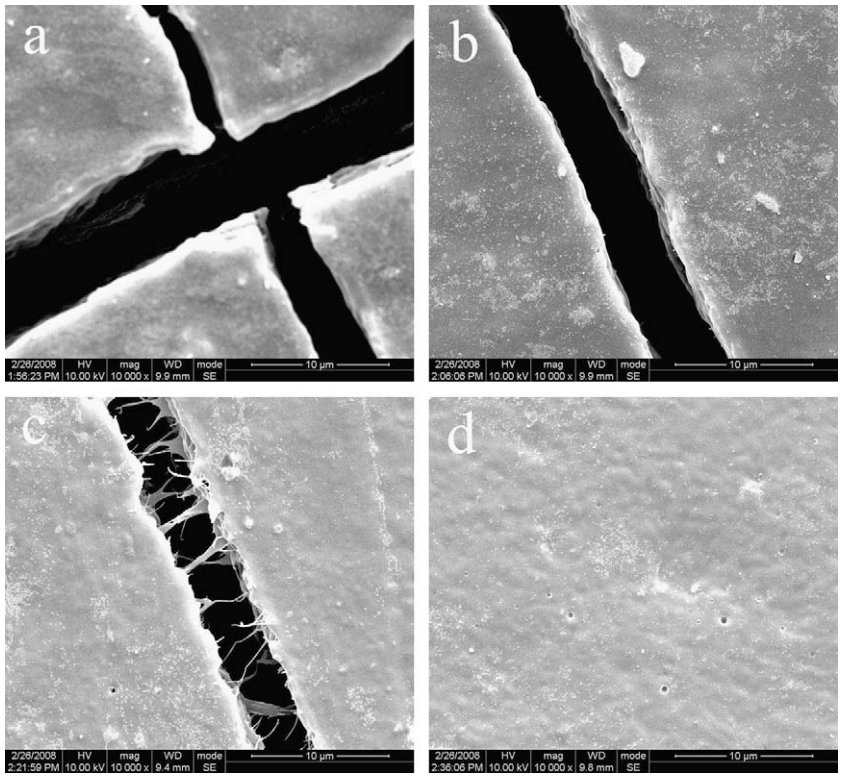

Fig. 10. SEM micrographs of PPDO-H (a), PPDOBS9 (b), PPDOBS7 (c) and PPDOBS5 (d) (magnification: 10000×) during the hydrolysis in phosphate buffer solution (pH 7.4) at 37 °C after 8 weeks.

degradation accelerated after 4th week, probably because of the autocatalysis of carboxyl groups [38].

Weight loss is a simple evaluation for the hydrolysis progress of polymers during the exposure to the hydrolytic medium. Fig. 8 shows the retention weight of the samples as a function of the degradation time. The retention weight of PPDO-H decreased rapidly after 4 weeks, and had a weight loss of 16 ± 2% at 10th week. This result is lower than that reported by Sabino et al. [36] who found a weight loss of 25% after 10 weeks of degradation in phosphate buffer solution of pH 7.44 at 37 °C. It may be ascribed to the incorporation of chain-extender, since it has been reported that the presence of urethane bonds in the chain-extended polyesters makes them degrade slower than the original polyesters [39]. During the period investigated, PPDO-H lost its weight faster than PPDOBS copolymers, especially after 4 weeks, and a final weight loss of 36 ± 3% was gotten after 18 weeks. While the weight loss of PBS-H remains almost unchanged during the course of hydrolytic degradation, and only varied within 3%. After 18 weeks, the final weight loss of PPDOBS9, PPDOBS7, PPDOBS5 and PPDOBS2 were 31 ± 2, 19 ± 2, 17 ± 1 and 8 ± 1%, respectively. The weight loss increased with the degradation time for PPDOBS copolymers, and decreased with increasing the weight fraction of PBS blocks.

From the above results, it can be seen that the hydrolytic degradation rate of PPDOBS could be controlled by adjusting the weight fraction of PPDO and PBS blocks in the copolymers.

3.4.2. Scanning electronic microscopy

While the hydrolysis progresses, the fragments of chains involved in the hydrolysis can migrate into the aqueous medium, leaving empty spaces on the surface of the sample. The cracks on the surface can be detected by SEM [36]. For the different hydrolysis properties of PPDO and PBS blocks, some morphological differences probably exist among the copolymers as the hydrolysis proceeds. Fig. 9 and Fig. 10 show the SEM micrographs of PPDO-H, PPDOBS9, PPDOBS7 and PPDOBS5 after various degradation time. After 8 weeks, some cracks were detected on the surface of PPDO-H, and there was only one crack for PPDOBS9 and PPDOBS7. While for PPDOBS5, no cracks were observed on the surface. When the micrographs of the cracks were magnified 10,000 times (Fig. 10), some filaments connecting the both side of the cracks can be observed for PPDOBS7. With further degradation, the number of the cracks increased. But for PPDOBS5, no cracks were detected even after 14 weeks. The physical integrity of the samples became better with increasing the weight fraction of PBS blocks in the copolymers. The surface morphologic changes also indicate that the hydrolytic degradation can be controlled by changing the weight fraction of PPDO and PBS blocks.

3.4.3. Thermal analysis

The ester bonds in the aliphatic polyesters are sensitive when suffering from water. Their cleavage occurs first in the amorphous areas during the hydrolytic degradation. The short chains involved in the breaking can incorporate into the crystal, causing an increase in crystallization at the initial stage of hydrolysis; at the later stage of hydrolysis, most of hydrolysis occurs in the crystal regions and gradually destroys these regions [36,37,40,41]. In this section, the crystallization in the hydrolytic degradation process has been investigated. The samples of PPDO-H, PPDOBS7 and PBS-H were characterized by DSC to evaluate the variation of melting peak temperature (T_m) and melting enthalpy (ΔH_m) as a function of the degradation time. The degrees of crystallization (X_c) was calculated by Eq. (3). Fig. 11 shows the DSC heating curves of PPDO-H, PPDOBS7, and PBS-H. The corresponding data obtained from DSC curves were listed in Table 4. As can be observed, T_m, ΔH_m, and X_c increased with the degradation time. After 9 weeks, the melting point of PPDO-H increased from 84.4 to 96.0 °C, and the corresponding value of PBS-H increased from 106.6 to 109.1 °C. The melting point of PPDO blocks in PPDOBS7 increased from 84.8 to 94.7 °C, while that of PBS blocks increased from 103.5 to 109.3 °C.

It can be also seen that X_c of PPDO-H increased from 8.0% to 39.2% after 9 weeks, while the corresponding crystallinity of PPDO blocks in PPDOBS7 increased from 24.9% to 29.4%. With respect to PBS blocks in PPDOBS7 and PBS-H, the initial degrees of crystallization were 31.2% and 31.8%, and increased to 39.1% and 39.3%, respectively, after 9 weeks. The increase in crystallinity can be explained by the "cleavage-induced crystallization" mechanism [42,43]. When water diffuses into the samples, the attack happens on both amorphous and crystalline areas, but preferentially on the amorphous areas because of their less density. Then chain scission occurs and subsequently results in less entangled chain segments. These short segments can organize themselves to the crystal at the employed hydrolysis temperature (above the T_g of PPDO and PBS), which causes an increase in crystallinity.

4. Conclusions

PPODBS copolymers with different composition were prepared through a two-step process including preparation of PPDO-OH and PBS-OH prepolymers and the following copolymerization of the two kinds of prepolymers by coupling with HDI. The molecular structures of the prepared prepolymers and copolymers were characterized by means of ^{1}H NMR. Compared with the prepolymers, the intrinsic viscosities of PPDOBS copolymers increased by 10 times at least. WAXD analysis showed that the crystalline form of PPDO and PBS blocks in the copolymers was the same as that of the corresponding homopolymer. POM analysis indicated that PBS blocks crystallized first and acted as a nucleating agent for PPDO blocks crystallization. The crystallization rate of PPDOBS copolymers increased with increasing the weight fraction of PBS blocks. The appearance of one T_g and two T_m detected by DSC suggested that PPDO and PBS blocks were compatible in the amorphous regions but separated in the crystal domains. During the hydrolytic degradation, the pH value, water absorption, retention weight, and physical integrity varied regularly with increasing the weight fraction of PBS blocks. All the

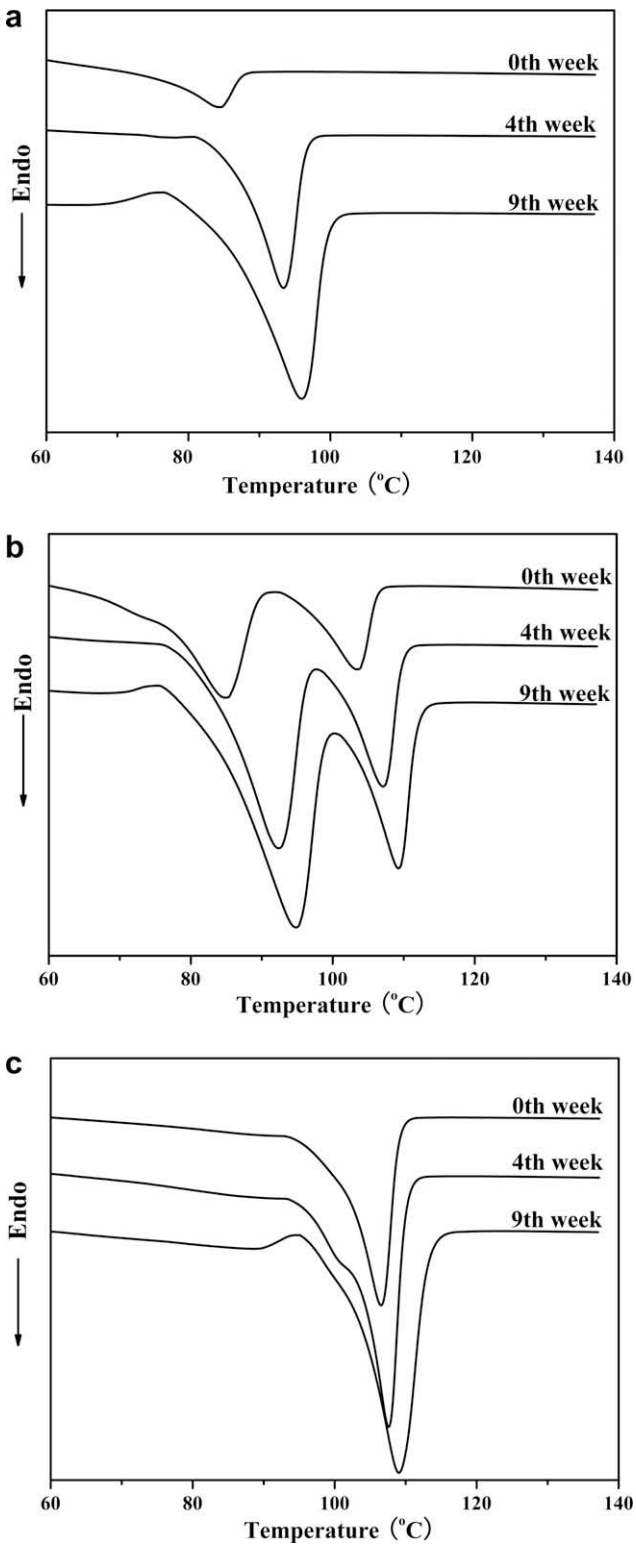

Fig. 11. DSC heating curves of PPDO-H (a), PPDOBD7 (b) and PBS-H (c) during the hydrolysis in phosphate buffer solution (pH 7.4) at 37 °C.

results of hydrolytic degradation showed that the hydrolytic degradation rate of PPDOBS could be controlled by adjusting the weight fraction of PPDO and PBS blocks in the copolymers.

Table 4
DSC data of PPDO-H, PBS-H and PPDOBS copolymers obtained from the heating curves during the hydrolysis in phosphate buffer solution (pH 7.4) at 37 °C.

Sample	Time (weeks)	T_m[a] (°C)	ΔH_m[a] (J/g)	X_c[a] (%)	T_m[b] (°C)	ΔH_m[b] (J/g)	X_c[b] (%)
PPDO-H	0	84.4	11.3	8.0	–	–	–
	4	93.4	46.2	32.8	–	–	–
	9	96.0	55.3	39.2	–	–	–
PPDOBS7	0	84.8	24.6	24.9	103.5	10.3	31.2
	4	92.3	25.3	25.6	107.2	11.8	35.7
	9	94.7	29.0	29.4	109.3	12.9	39.1
PBS-H	0	–	–	–	106.6	35.0	31.8
	4	–	–	–	107.6	37.6	34.2
	9	–	–	–	109.1	43.2	39.3

[a] The value of PPDO blocks in the copolymer.
[b] The value of PBS blocks in the copolymer.

Acknowledgments

This work was supported by the National Science Fund for Distinguished Young Scholars (50525309) and the WAXD and ^{1}H NMR analyses were provided by the Analytical and Testing Center of Sichuan University.

References

[1] Yang KK, Wang XL, Wang YZ. Poly(*p*-dioxanone) and its copolymers. J Macromol Sci Polym Rev 2002;C42:373–98.
[2] Gertzman A, Thompson DR. Annealed polydioxanone surgical device and method for producing the same. US Patent 4 591 630, 1986.
[3] Bezwada RS, Shalaby SW, Koelmel DF. Copolymers of (*p*-dioxanone/glycolide and/or lactide) and *p*-dioxanone. US Patent 5 470 340, 1995.
[4] Wang H, Dong JH, Qiu KY, Gu ZW. Synthesis of poly(1,4-dioxan-2-one-co-trimethylene carbonate) for application in drug delivery systems. J Polym Sci A Polym Chem 1998;36(8):1301–7.
[5] Forschner TC. Process for preparing para-dioxanones. US Patent 5 310 945, 1994.
[6] Doddi N, Versfelt CC, Wasserman D. Synthetic absorbable surgical devices of polydioxanone. US Patent 4 032 988, 1977.
[7] Lipinsky ES, Sinclair RG, Browing JD. Degradable polydioxaneone based materials. US Patent 5 767 222, 1997.
[8] Nishida H, Yamashita M, Hattori T, Endo T, Tokiwa Y. Thermal decomposition of poly(1, 4-dioxan-2-one). Polym Degrad Stab 2000;70(3):485–96.
[9] Ding SD, Bai CY, Liu ZP, Wang YZ. Enhanced thermal stability of poly(*p*-dioxanone) in melt by adding an end-capping reagent. J Therm Anal Calorim 2008;94(1):89–95.
[10] Ding SD, Liu ZP, Yang T, Zheng GC, Wang YZ. Effect of polycarbodiimide on the thermal stability and crystallization of poly(*p*-dioxanone). J Polym Res 2009. doi:10.1007/s10965-009-9290-y [published online on April 4, 2009].
[11] Ding SD, Wang YZ. Enhanced thermal stability of poly(1,4-dioxan-2-one) in melt by adding a chelator. Polym Degrad Stab 2006;91(10):2465–70.
[12] Libiszowski J, Kowalski A, Szymanski R, Duda A, Raquez JM, Degee P, et al. Monomer-linear macromolecules-cyclic oligomers equilibria in the polymerization of 1,4-dioxan-2-one. Macromolecules 2004;37(1):52–9.
[13] Nishida H, Yamashita M, Endo T, Tokiwa Y. Equilibrium polymerization behavior of 1,4-dioxan-2-one in bulk. Macromolecules 2000;33(19):6982–6.
[14] Sabino MA, Feijoo JL, Muller AJ. Crystallisation and morphology of neat and degraded poly(*p*-dioxanone). Polym Degrad Stab 2001;73(3):541–7.
[15] Liu ZP, Ding SD, Sui YJ, Wang YZ. Enhanced hydrolytic stability of poly(*p*-dioxanone) with polycarbodiimide. J Appl Polym Sci 2009;112(5):3079–86.
[16] Raquez JM, Degee P, Narayan R, Dubois P. Some thermodynamic, kinetic, and mechanistic aspects of the ring-Opening polymerization of 1,4-dioxan-2-one initiated by Al(OiPr)$_3$ in bulk. Macromolecules 2001;34(24):8419–25.
[17] Raquez JM, Degee P, Narayan R, Dubois P. Synthesis of melt-stable and semi-crystalline poly(1,4-dioxan-2-one) by ring-opening (co)polymerisation of 1,4-dioxan-2-one with different lactones. Polym Degrad Stab 2004;86(1):159–69.
[18] Li B, Chen SC, Qiu ZC, Yang KK, Tang SP, Yu WJ, et al. Synthesis of poly(lactic acid-b-*p*-dioxanone) block copolymers from ring opening polymerization of *p*-dioxanone by poly(L-lactic acid) macroinitiators. Polym Bull 2008;61(2):139–46.
[19] Bahadur KCR, Bhattarai SR, Aryal S, Khil MS, Dharmaraj N, Kim HY. Novel amphiphilic triblock copolymer based on PPDO, PCL, and PEG: synthesis, characterization, and aqueous dispersion. Colloids Surf A: Physicochem Eng Aspects 2007;292(1):69–78.
[20] Zhang YH, Wang XL, Wang YZ, Yang KK, Li J. A novel biodegradable polyester from chain-extension of poly(*p*-dioxanone) with poly(butylene succinate). Polym Degrad Stab 2005;88(2):294–9.
[21] Kulkarni A, Reiche J, Hartmann J, Kratz K, Lendlein A. Selective enzymatic degradation of poly(ε-caprolactone) containing multiblock copolymers. Eur J Pharm Biopharm 2008;68(1):46–56.
[22] Lendlein A, Langer R. Elastic shape-memory polymers for potential biomedical applications. Science 2002;296(5573):1673–6.
[23] Li HY, Chang J, Cao AM, Wang JY. In vitro evaluation of biodegradable poly(butylene succinate) as a novel biomaterial. Macromol Biosci 2005;5(5):433–40.
[24] Annikam L, Albertsson AC, Hakkarainen M. Quantitative determination of degradation products an effective means to study early stages of degradation in linear and branched poly(butylene adipate) and poly(butylene succinate). Polym Degrad Stab 2004;83(3):487–93.
[25] Jeong EH, Im SS, Youk JH. Electrospinning and structural characterization of ultrafine poly(butylene succinate) fibers. Polymer 2005;46(23):9538–43.
[26] Zeng Q, Yang KK, Chen SC, Wang XL, Zeng JB, Wang YZ. A new approach to prepare high molecular weight poly(*p*-dioxanone) by chain-extending from dihydroxyl terminated propolymers. Eur Polym J 2008;44(2):465–74.
[27] Tezuka Y, Ishii N, Kasuya K, Mitomo H. Degradation of poly(ethylene succinate) by mesophilic bacteria. Polym Degrad Stab 2004;84(1):115–21.
[28] Hiltunen K, Seppala JV, Harkonen M. Lactic acid based poly(ester-urethanes): use of hydroxyl terminated prepolymer in urethane synthesis. J Appl Polym Sci 1997;63(8):1091–100.
[29] Ba CY, Yang J, Hao QH, Liu XY, Cao AM. Syntheses and physical characterization of new aliphatic triblock poly(L-lactide-b-butylene succinate-b-L-lactide)s bearing soft and hard biodegradable building blocks. Biomacromolecules 2003;4(6):1827–34.
[30] Hoffman JD, Davis GT, Lauriten JI. Treatise on solid state chemistry. In: Hannay NB, editor. New York: Plenum Press; 1976. p. 497–614.
[31] Wang XL, Yang KK, Wang YZ, Chen DQ, Chen SC. Crystallization and morphology of starch-g-poly(1,4-dioxan-2-one) copolymers. Polymer 2004;45(23):7961–8.
[32] Albuerne J, Marquez L, Mu1ller AJ, Raquez JM, Degee P, Dubois P, et al. Nucleation and crystallization in double crystalline poly(*p*-dioxanone)-b-poly(ε-caprolactone) diblock copolymers. Macromolecules 2003;36(5):1633–44.
[33] Muller AJ, Albuerne J, Marquez L, Raquez JM, Degee P, Dubois P, et al. Self-nucleation and crystallization kinetics of double crystalline poly(*p*-dioxanone)-b-poly(ε-caprolactone) diblock copolymers. Faraday Discuss 2005;128(10):231–52.

[34] Ishikiriyama K, Pyda M, Zhang G, Forschner T, Grebowicz J, Wunderlich B. Heat capacity of poly-*p*-dioxanone. J Macromol Sci Phys 1998;37(1):27–44.
[35] Nikolic MS, Djonlagic J. Synthesis and characterization of biodegradable poly(butylene succinate-co-butylene adipate). Polym Degrad Stab 2001;74(2):263–70.
[36] Sabino MA, Gonzalez S, Marquez L, Feijoo JL. Study of the hydrolytic degradation of polydioxanone PPDX. Polym Degrad Stab 2000;69(2):209–16.
[37] Sabino MA, Albuerne J, Muller AJ, Brisson J, Prudhomme RE. Influence of in vitro hydrolytic degradation on the morphology and crystallization behavior of poly(*p*-dioxanone). Biomacromolecules 2004;5(2):358–70.
[38] Nishida H, Yamashita M, Nagashima M, Hattori N, Endo T, Tokiwa Y. Theoretical prediction of molecular weight on autocatalytic random hydrolysis of aliphatic polyesters. Macromolecules 2000;33(17):6595–601.
[39] Shirahama H, Kawaguchi Y, Aludin MS, Yasuda H. Synthesis and enzymatic degradation of high molecular weight aliphatic polyesters. J Appl Polym Sci 2001;80(3):340–7.
[40] Lin HL, Chu CC, Grubb D. Hydrolytic degradation and morphologic study of poly-*p*-dioxanone. J Biomed Mater Res 1993;27(2):153–66.
[41] Ooi CP, Cameron RE. The hydrolytic degradation of polydioxanone (PDSII) sutures. Part I: morphological aspects. J Biomed Mater Res (Appl Biomater) 2002;63(3):280–90.
[42] Chu CC. Hydrolytic degradation of polyglycolic acid: tensile strength and crystallinity study. J Appl Polym Sci 1981;26(5):1727–34.
[43] Zong XH, Wang ZG, Hsiao BS, Chu B. Structure and morphology changes in absorbable poly(glycolide) and poly(glycolide-co-lactide) during in vitro degradation. Macromolecules 1999;32(24):8107–14.